Allergy Asthma Immunol Res. 2025 Jan;17(1):111-126
https://doi.org/10.4168/aair.2025.17.1.111
pISSN 2092-7355·eISSN 2092-7363

Allergy, Asthma & Immunology Research AAIR

Original Article

Peroxisome Metabolism Pathway and EHHADH Expression are Downregulated in Macrophages in Neutrophilic Asthma

Gongqi Chen,[1,2] **Wei Gu**,[1,2] **Chunli Huang**,[1,2] **Weiqiang Kong**,[1,2] **Lu Zhao**,[1,2] **Huiru Jie**,[1,2] **Guohua Zhen**[1,2*]

[1]Division of Respiratory and Critical Care Medicine, Department of Internal Medicine, Tongji Hospital, Tongji Medical College, Huazhong University of Science and Technology, Wuhan, China
[2]Key Laboratory of Respiratory Diseases, National Health Commission of People's Republic of China, and National Clinical Research Center for Respiratory Diseases, Wuhan, China

Received: Apr 7, 2024
Revised: Aug 26, 2024
Accepted: Sep 4, 2024
Published online: Oct 24, 2024

Correspondence to
Guohua Zhen, PhD
Division of Respiratory and Critical Care Medicine, Department of Internal Medicine, Tongji Hospital, Tongji Medical College, Huazhong University of Science and Technology, No.1095 Jie Fang Avenue, Hankou, Wuhan 430030, China.
Tel: +86-27-83669809
Fax: +86-27-83662640
Email: ghzhen@tjh.tjmu.edu.cn

ORCID iDs
Gongqi Chen
https://orcid.org/0009-0009-4860-1335
Guohua Zhen
https://orcid.org/0000-0001-5582-7900

Disclosure
There are no financial or other issues that might lead to conflict of interest.

ABSTRACT

Purpose: Neutrophilic asthma (NA) is associated with more severe symptoms and poor responsiveness to inhaled corticosteroid therapy. Macrophages are the most abundant immune cells in the airway, but the role of macrophages in NA pathogenesis has not been fully studied. We hypothesized that dysregulation of peroxisome metabolism in macrophages may drive NA.
Methods: We retrieved microarray datasets from the GEO Gene Expression Omnibus database by using induced sputum samples from eosinophilic and neutrophilic asthma patients as well as healthy controls. We identified key molecules in NA and validated the expression of the key genes in our cohort of asthma patients using quantitative polymerase chain reaction (PCR). Furthermore, immunofluorescence staining was performed to detect the expression and localization of the key molecule in bronchoalveolar lavage (BAL) cells from asthma patients and the murine model of neutrophilia-dominant allergic airway inflammation. The expression of the key molecule was also examined in mouse bone marrow-derived macrophages (BMDMs) by quantitative PCR and western blotting.
Results: Enoyl-CoA hydratase and 3-hydroxyacyl CoA dehydrogenase (EHHADH), sterol carrier protein 2, and peroxisomal biogenesis factor 14 were identified as the key molecules and were downregulated in patients with NA or severe asthma. The peroxisomal fatty acid metabolism pathway was significantly downregulated in NA. In our cohort of asthma patients, the expression of EHHADH, a key enzyme of the peroxisomal fatty acid beta-oxidation, was significantly decreased in non-eosinophilic asthma patients and positively correlated with airflow limitation. EHHADH was primarily expressed in macrophages in BAL cells. EHHADH was downregulated in lipopolysaccharide (LPS)-induced M1-like macrophages in mouse BMDMs. Fenofibrate, an agonist of the peroxisome pathway, significantly inhibits LPS-induced macrophage M1 polarization.
Conclusions: EHHADH expression and the peroxisome metabolism pathway are downregulated in macrophages in patients with NA. This downregulation may contribute to macrophage M1 polarization and neutrophilic airway inflammation in asthma.

Keywords: Asthma; neutrophils; macrophages; peroxisomes; EHHADH protein; PEX14 protein; sterol carrier protein 2

Allergy, Asthma & Immunology Research AAIR

INTRODUCTION

Asthma is a chronic airway inflammatory disease characterized by airway hyperresponsiveness, reversible airflow restriction, excessive mucus production, and remodeling of the airway walls.[1] Asthma currently affects about 358 million people globally and is 1 of the top 5 respiratory diseases threatening global health.[2,3] Severe asthma imposes significant economic and healthcare burdens on both individuals and society.[4] Severe asthma can be fatal and, in some cases, is characterized by neutrophilic airway inflammation.

Asthma is divided into 4 different inflammatory phenotypes based on the number of inflammatory cells in induced sputum: eosinophilic asthma (EA), neutrophilic asthma (NA), mixed granulocytic asthma, and paucigranulocytic asthma.[5] NA is characterized by having more than 61% neutrophils in induced sputum.[6] Frequent attacks and severe symptoms are hallmarks of NA.[7] Although inhaled corticosteroids (ICS) are commonly used in the clinical treatment of asthma, NA exhibits poor responsiveness to ICS. Therefore, it is crucial to understand the pathogenesis of NA.[8]

Macrophages are crucial in the development of allergic airway inflammation in asthma.[9,10] Macrophage exhibits 2 distinct activated states known as M1 (classically activated) and M2 (alternatively activated) polarization.[11] M1 macrophages promote inflammation, while M2 macrophages have anti-inflammatory functions, with M2 polarization being linked to EA and M1 polarization to NA.[12-14]

Peroxisomes are organelles found in nearly all eukaryotic cells, playing key roles in cell metabolism, including fatty acid beta-oxidation, ether glycerin plasma synthesis, and oxidation-reduction reaction homeostasis.[15,16] Abnormal fatty acid metabolism is involved in the pathogenesis of asthma. However, the role of fatty acid metabolism in NA remains unclear.[17]

In this study, we aimed to identify the key signaling pathway in NA by analyzing sputum cell datasets from EA and NA patients obtained from the Gene Expression Omnibus (GEO) database.

MATERIALS AND METHODS

Microarray dataset acquisition and differentially expressed genes (DEGs) identification

We obtained the GSE41863 dataset from GEO (http://www.ncbi.nlm.nih.gov/geo) utilizing the getGEO function of the GEOquery package (version 2.58.0) in R software (version 4.0.4), which includes 9 control samples, 15 EA samples and 17 NA samples. Next, we based on R limma software package (version 3.46.0) empirical Bayes method ($P < 0.05$, $|\log FC| > 1$) to identify DEGs between EA and NA groups. Volcano and heat maps were generated using an online platform (https://www.bioinformatics.com.cn) for data analysis and visualization.

Protein-protein interaction (PPI) network construction and hub genes validation

DEGs were used to construct the PPI network via the STRING database (http://www.string-db.org/), applying a cut-off interaction score of > 0.4. The PPI network was visualized using Cytoscape software (version 3.6.1). The top 10 hub genes in the PPI network were identified using the maximal clique centrality (MCC) method in the Cytohubba plugin.

https://doi.org/10.4168/aair.2025.17.1.111

Functional and pathway enrichment analyses

Gene Ontology (GO) and Kyoto Encyclopedia of Genes and Genomes (KEGG) pathway enrichment analyses were conducted and visualized using the clusterProfiler package (version 3.18.1) in R software. Gene Set Enrichment Analysis (GSEA) was performed using GSEA software (version 4.1.0). KEGG was selected as the gene pool. Gene sets were considered significantly enriched if the *P* value was < 0.05 and the false discovery rate (FDR) was < 25%, with 1,000 permutations per analysis. GSEA parameters were set as follows: The parameter "Collapse data set to gene symbols" is set to "false". The parameter "Permutation type" is set to "phenotype". The parameter "Enrichment statistic" is set to "weighted", while the parameter "Metric for ranking genes" is set to "Singal2Noise".

Human subjects

Induced sputum samples were collected from 10 healthy controls, 21 EA patients (sputum eosinophils > 3%), and 18 non-EA patients (sputum eosinophils < 3%). All participants were Chinese and recruited from Tongji Hospital. None of the participants had ever smoked or received inhaled or oral corticosteroid or leukotriene antagonists. For each subject, we recorded demographic data, collected induced sputum, measured spirometry without bronchodilator, assessed fractional exhaled nitric oxide (FeNO) levels, and analyzed serum immunoglobulin E (IgE). All asthma patients had a history of episodic wheezing and had an accumulated dosage of methacholine that resulted in a 20% decrease (PD20) in forced expiratory volume in the first second (FEV1) of less than 2.505 mg and/or a 12% or greater increase in FEV1 following the inhalation of 200 μg of salbutamol. We collected bronchoalveolar lavage fluid (BALF) in a subset of healthy controls (n = 10) and asthma patients (n = 36). EA was defined as the induced sputum cell count with eosinophils greater than 3% and neutrophils less than 61%. Non-EA patients are defined as induced sputum eosinophil percentage below 3%. Healthy controls are defined as individuals with no history of smoking, allergies, or respiratory diseases, with normal pulmonary function, and without airway hyperresponsiveness. Written informed consent was obtained from all subjects. The ethics committee of Tongji Hospital, Huazhong University of Science and Technology approved the study.

Mouse model of neutrophilia-dominant allergic airway inflammation

Female C57BL/6J mice aged 6 to 8 weeks were divided into 2 groups: the control group and the neutrophilia-dominant allergic airway inflammation group (ovalbumin [OVA]/LPS). In the OVA/LPS group, the mice were sensitized through intranasal administration of 75 μg OVA and 10 μg LPS in 40 μL saline on days 0, 1, 2, and 7. They were challenged with intranasal administration of 50 μg OVA in 40 μL saline on days 14, 15, 21, and 22. The mice in the control group were sensitized with an equal volume of normal saline. Twenty-four hours after the final OVA challenge, lung tissues and BALF were collected for real-time quantitative polymerase chain reaction (PCR) and immunofluorescence analysis. The ethical approval for the animal experiments was obtained from the ethics committee of Tongji Hospital, Huazhong University of Science and Technology.

Real-time PCR

Total RNA from induced sputum cells, BAL cells, mouse lungs, and bone marrow-derived macrophage (BMDM) cells were isolated by TRIzol (Takara, Tokyo, Japan) and reversed transcription into cDNA by PrimeScript RT reagent kit (Takara). All the primer sequences were obtained from the PrimerBank database and listed in **Supplementary Table S1**. The expression of these genes was determined by the $2^{-\Delta\Delta CT}$ method. Gene expression was expressed as log2 transformed and relative to the median of the control group.

https://doi.org/10.4168/aair.2025.17.1.111

Immunofluorescence

The immunofluorescence method of frozen slides was as follows: After the slides were restored to room temperature, they were washed 3 times with phosphate-buffered saline (PBS) for 5 minutes each time. The immunostaining permeabilization buffer was added and incubated at room temperature for 20 minutes. The goat serum-blocking buffer was added and blocked for 30 minutes. Subsequently, the slices were incubated with EHHADH (1:200) and CD68 (1:200) antibodies in a wet box overnight at 4°C. Antibody wash buffer was added to remove the primary antibody, and then the antibody wash buffer was added and incubated at room temperature for 1 hour. After PBS cleaning, 4′,6-diamidino-2-phenylindole (DAPI) staining is used. Washing again, the slices were sealed with an anti-fluorescence quenching sealing agent. Then, slices were observed under a fluorescence microscope within 1 week to avoid fluorescence quenching, and images were collected.

Western blot

For protein sample preparation, the following steps were taken: The cells were lysed in ice-cold RIPA lysis buffer (Beyotime, Shanghai, China), supplemented with EDTA-free Protease Inhibitor Cocktail Tablets (Roche, Basel, Switzerland). The lysates were then subjected to 8% sodium dodecyl-sulfate polyacrylamide gel electrophoresis (SDS-PAGE) or non-reducing SDS-PAGE for protein separation. The proteins were subsequently electrophoretically transferred onto a polyvinylidene difluoride (PVDF) membrane (Millipore, Billerica, MA, USA). Next, the PVDF membranes were blocked in Tris-buffered saline (pH 7.4) containing 0.1% Tween-20 (Sigma-Aldrich, St. Louis, MO, USA) and 5% (w/v) nonfat milk. The membranes were then incubated overnight at 4°C in 5% milk with specific antibodies for the targeted proteins. The antibodies used were rabbit anti-EHHADH mAb (1:1,000; Abmart, Shanghai, China) and anti-iNOS mAb (1:1,000; Abcam, Cambridge, UK). After the overnight incubation, the membranes were exposed to a horseradish peroxidase-conjugated goat anti-rabbit secondary antibody (1:4,000; Servicebio, Wuhan, China) for 1 hour at room temperature. The protein signals were detected using an ECL kit (MCE, Monmouth Junction, NJ, USA) following the manufacturer's instructions.

Statistical analysis

The data analysis was performed using Prism version 8 (GraphPad Software, San Diego, CA, USA). For data that followed a normal distribution, we calculated the means ± standard deviation and conducted parametric tests such as Student's *t*-test or one-way analysis of variance followed by Tukey's multiple comparison test to compare between groups. For non-normally distributed data, medians and interquartile ranges were calculated, and non-parametric tests such as the Mann-Whitney *U* test were employed. Spearman's rank correlation coefficient was performed to assess correlation. A *P* value less than 0.05 was considered statistically significant.

RESULTS

EHHADH, sterol carrier protein 2 (SCP2), and peroxisomal biogenesis factor 14 (PEX14) are hub molecules in NA

We selected the GSE41863 dataset from the GEO database, which analyzed the sputum samples from 9 healthy controls, 15 EA and 17 NA patients. Using the "Limma" package ($P < 0.05$, $|\log FC| > 1$), we identified 1,077 DEGs in the comparison between EA vs. control (723 upregulated and 356 downregulated), and 1,079 DEGs between EA vs. NA (655

https://doi.org/10.4168/aair.2025.17.1.111

upregulated and 422 downregulated) (**Supplementary Fig. S1A and B**). To further identify the dysregulated genes in the NA group, we focused on the 760 overlapped DEGs between NA vs. control and NA vs. EA (**Fig. 1A**). The enriched GO and KEGG analyses of the 760 DEGs were performed and visualized with the clusterProfiler package in R software. GO biological process (BP) enrichment analysis identified processes such as neutrophil degranulation and activation involved in immune response, small molecule catabolic process, cell chemotaxis and fatty acid catabolic process (**Supplementary Fig. S1C**). For the cellular component (CC), DEGs were significantly enriched in specific and tertiary granules and secretory granule membranes (**Supplementary Fig. S1D**). For molecular function (MF), DEGs were significantly

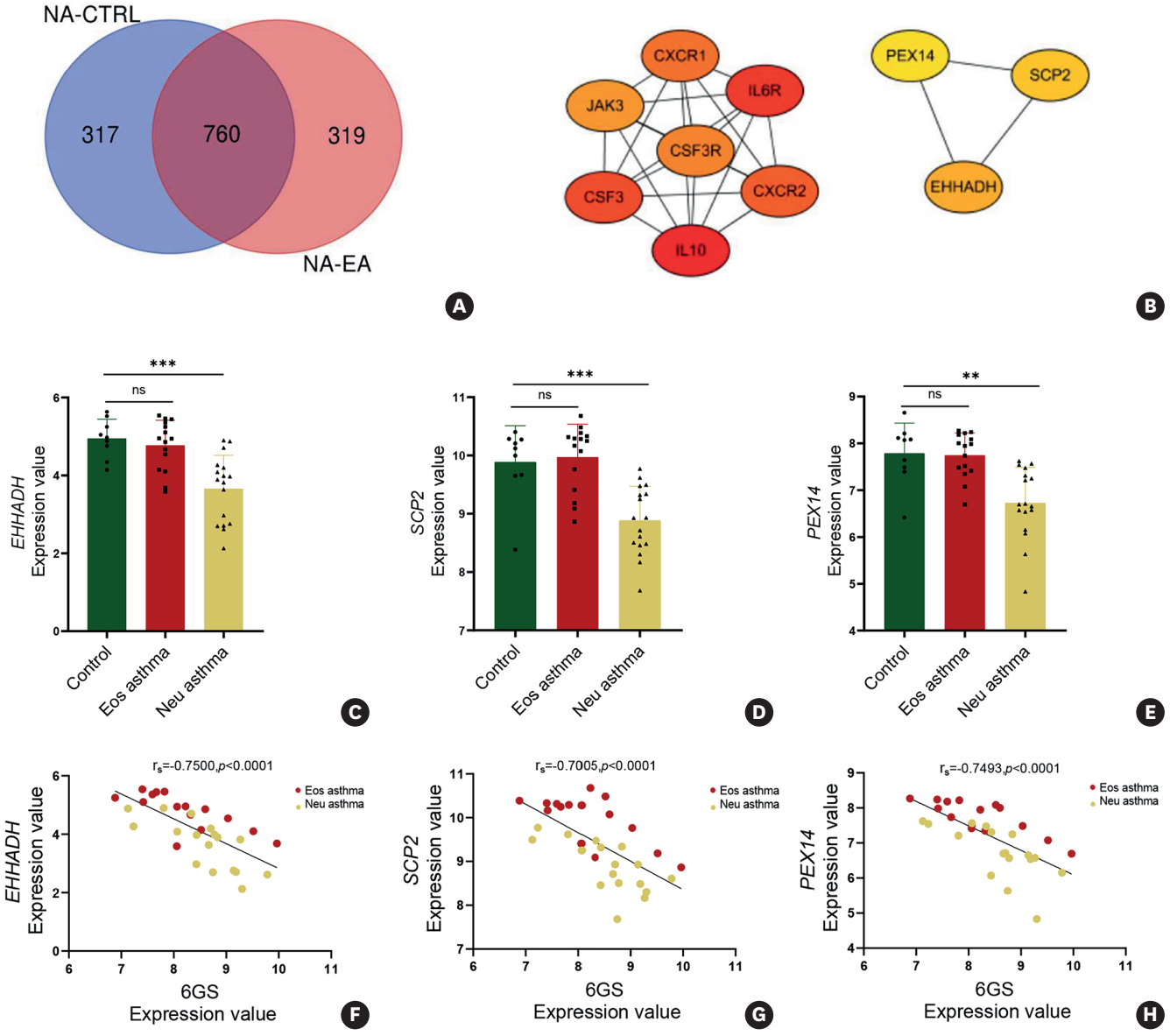

Fig. 1. EHHADH, SCP2, and PEX14 are hub molecules in sputum cells from NA patients. (A) DEGs between NA vs. control subjects, and NA vs. EA were shown using a Venn diagram. (B) The top 10 hub molecules in DEGs were identified with the Cytohubba plugin. (C-E) The expression value of *EHHADH*, *PEX14*, and *SCP2* in the dataset GSE41863. (F-H) Spearman's correlation assays between EHHADH, PEX14, SCP2 expression value and 6GS expression value.
EHHADH, enoyl-CoA hydratase and 3-hydroxy acyl CoA dehydrogenase; SCP2, sterol carrier protein 2; PEX14, peroxisomal biogenesis factor 14; DEG, differentially expressed gene; NA, neutrophilic asthma; EA, eosinophilic asthma; 6GS, 6-gene signature; CTRL, healthy controls; CXCR, CXC motif chemokine receptor; CSF, colony-stimulating factor; IL, interleukin; ns, not significant.
$^{**}P < 0.01$, $^{***}P < 0.001$.

https://doi.org/10.4168/aair.2025.17.1.111

enriched in cytokine receptor activity, NAD binding and NAD(P)+ nucleosidase activity (**Supplementary Fig. S1E**). KEGG pathway analysis demonstrated that DEGs were strongly involved in cytokine-cytokine receptor interaction, pantothenate and CoA biosynthesis, and viral protein interaction with cytokine and cytokine receptors (**Supplementary Fig. S1F**).

To identify the hub molecules in the NA group, the PPI network was constructed using the STRING database and visualized with Cytoscape software. The top 10 hub molecules in overlapped DEGs were confirmed by the MCC computing method with the Cytohubba plugin via the PPI network, which included interleukin 6 receptor (IL6R), interleukin 10 (IL10), colony-stimulating factor (CSF) 3, CXC motif chemokine receptor (CXCR) 2, CSF3R, CXCR1, JAK3, EHHADH, SCP2, and PEX14 (**Fig. 1B**). IL6R, IL10, CSF3, CXCR2, CSF3R, CXCR1, and JAK3 were upregulated in the NA group (**Supplementary Fig. S2**). These molecules were widely connected with each other and are related to type 1 inflammation. EHHADH, SCP2, and PEX14 were closely interlinked. Compared to the control group, the expression of these 3 genes was significantly decreased in patients with NA, but not in patients with EA (**Fig. 1C-E**). EHHADH, SCP2, and PEX14 are involved in the peroxisome and fatty acid metabolism pathways, though the role of these pathways in NA has yet to be explored.

EHHADH, SCP2, and PEX14 are associated with asthma exacerbation and severity

Patients with NA exhibit more severe clinical symptoms and have a higher risk of asthma exacerbation. We subsequently analyzed the relationship between. between the risk of asthma exacerbation and the EHHADA/SCP2/PEX4 expression. A previous study identified a 6-gene signature, including *CLC*, *IL1B*, *CXCR2*, *CPA3*, *DNASE1L3*, and *ALPL*, in induced sputum to predict asthma exacerbation.[18] Our analysis showed that the 6-gene signature was significantly elevated in the NA group compared to the control group in dataset GSE41863 (**Supplementary Fig. S3**). Additionally, the expression levels of EHHADH, PEX14, and SCP2 were strongly negatively correlated with the 6-gene signature (**Fig. 1F-H**). This suggests that the downregulation of EHHADH, PEX14, and SCP2 is associated with asthma exacerbation.

To investigate whether the expression of EHHADH, SCP2, and PEX14 is associated with asthma severity, we utilized another dataset, GSE76262, which includes induced sputum cell microarray data from control subjects, and patients with moderate and severe asthma. We found that the expression levels of EHHADH and SCP2 were significantly decreased in patients with severe asthma compared to the control subjects. The expression of PEX14 was decreased but showed no statistical significance ($P = 0.09$) in patients with severe asthma compared to the control subjects. However, no significant differences in the expression levels of EHHADH, SCP2, and PEX14 were observed between patients with moderate asthma and control subjects (**Supplementary Fig. S4**). These findings suggest that the downregulation of EHHADH, SCP2, and PEX14 in induced sputum cells is associated with asthma severity.

EHHADH expression is downregulated in non-EA and correlated with airflow limitation

To validate our findings from GEO datasets, we collected induced sputum and BAL cells from 10 healthy controls, 21 EA patients (sputum eosinophils > 3%), and 18 non-EA patients (sputum eosinophil < 3%) to measure the expression of *EHHADH*, *SCP2*, and *PEX14*. The characteristics of subjects are summarized in **Table**. Compared to the control group, the mRNA level of *EHHADH* was significantly decreased in sputum cells from non-EA patients (**Fig. 2A**). However, no significant differences were observed in the expression levels of *PEX14*

https://doi.org/10.4168/aair.2025.17.1.111

Table. Subject characteristics

Characteristics	Controls	EA	Non-EA	*P* value (control vs. asthma)	*P* value (EA vs. non-EA)
Number	12	21	18		
Age (yr)	41.25 ± 8.91	41.62 ± 9.25	46.50 ± 10.86	0.43	0.14
Sex				0.34	> 0.99
Ratio of M:F	7:5	9:12	7:11		
% of female	58.33	42.86	38.89		
Body mass index (kg/m^2)	21.49 ± 3.38	24.11 ± 3.79	23.52 ± 3.26	0.06	0.62
FEV1% predicted	98.25 ± 11.42	83.91 ± 13.49	89.5 ± 16.33	0.03	0.26
FEV1%/FVC	0.81 ± 0.1	0.71 ± 0.09	0.67 ± 0.08	< 0.001	0.04
Sputum eosinophil (%)	4.18 ± 10.57	26.09 ± 19.43	1.364 ± 1.17	< 0.01	< 0.0001
Sputum neutrophil (%)	16.72 ± 23.63	18.41 ± 15.04	40.97 ± 28.99	0.14	< 0.01
Sputum macrophage (%)	73.62 ± 25.37	45.16 ± 27.41	45.66 ± 28.74	< 0.01	0.96
FeNO (ppb)	20.82 ± 8.976	110.9 ± 71.47	36.37 ± 34.30	0.02	< 0.001
Serum IgE (IU/mL)	55.68 ± 52.86	283.7 ± 470.1	116.1 ± 101.5	0.18	0.21
Blood eosinophil (%)	1.16 ± 1.27	7.45 ± 5.61	4.39 ± 3.92	0.05	< 0.0001
ACQ-5	-	14.43 ± 8.38	12.06 ± 6.75	-	0.56
ACT	-	15.33 ± 4.56	16.61 ± 4.2	-	0.37

Values were presented as mean ± standard deviation.
EA, eosinophilic asthma; M, male; F, female; FEV1, forced expiratory volume in the first second; FVC, forced vital capacity; FeNO, fraction of exhaled nitric oxide; IgE, immunoglobulin E; ACQ-5, asthma control questionnaire-5; ACT, asthma control test.

and *SCP2* between non-EA and controls (**Fig. 2B and C**). Furthermore, we found that the mRNA level of *EHHADH* was significantly positively correlated with the percentage of the FEV1 predicted value (FEV1% predicted) and FEV1%/forced vital capacity (FVC), which reflect the degree of airway obstruction (**Fig. 2D and E**). Moreover, the expression of *EHHADH* was positively correlated with the proportion of macrophages but not eosinophils or neutrophils in induced sputum, suggesting that *EHHADH* is predominantly expressed in macrophages (**Fig. 2F-H**). However, *EHHADH* levels in sputum cells did not show any correlation with FeNO and serum IgE (**Supplementary Fig. S5**). Additionally, the mRNA levels of EHHADH in BAL cells from the non-EA group exhibited a downward trend ($P = 0.16$) compared to the control group (**Supplementary Fig. S6A**).

We established a mouse model of neutrophilia-dominant allergic airway inflammation using OVA and LPS (**Supplementary Fig. S7**). Compared to saline-treated mice, the mRNA level of *Ehhadh* in lung tissue showed a decreasing trend but did not reach statistical significance ($P = 0.0594$) in mice with neutrophilia-dominant allergic airway inflammation (**Fig. 2I**). Our data suggest that EHHADH expression is downregulated in non-EA and is associated with airflow limitation.

The expression of EHHADH in macrophages is decreased in non-EA

Given the significant positive correlation between EHHADH expression and the proportion of macrophages in induced sputum, we further investigated EHHADH expression in macrophages. We performed immunostaining for EHHADH and CD68, a macrophage marker, in BAL cells obtained from eosinophilic/non-eosinophilic asthmatics and controls (**Fig. 3A**). We observed that EHHADH and CD68 staining were positive in the majority of BAL cells from control subjects. However, the number of EHHADH-positive cells was decreased in asthma patients, with a more pronounced decrease in non-EA. Compared to the control group, the relative fluorescence intensity of EHHADH/CD68 was significantly reduced in EA patients, with an even greater reduction in non-EA patients (**Fig. 3B**). A similar pattern was observed in the relative fluorescence intensity of EHHADH/DAPI (**Fig. 3C**).

https://doi.org/10.4168/aair.2025.17.1.111

Allergy, Asthma & Immunology Research AAIR

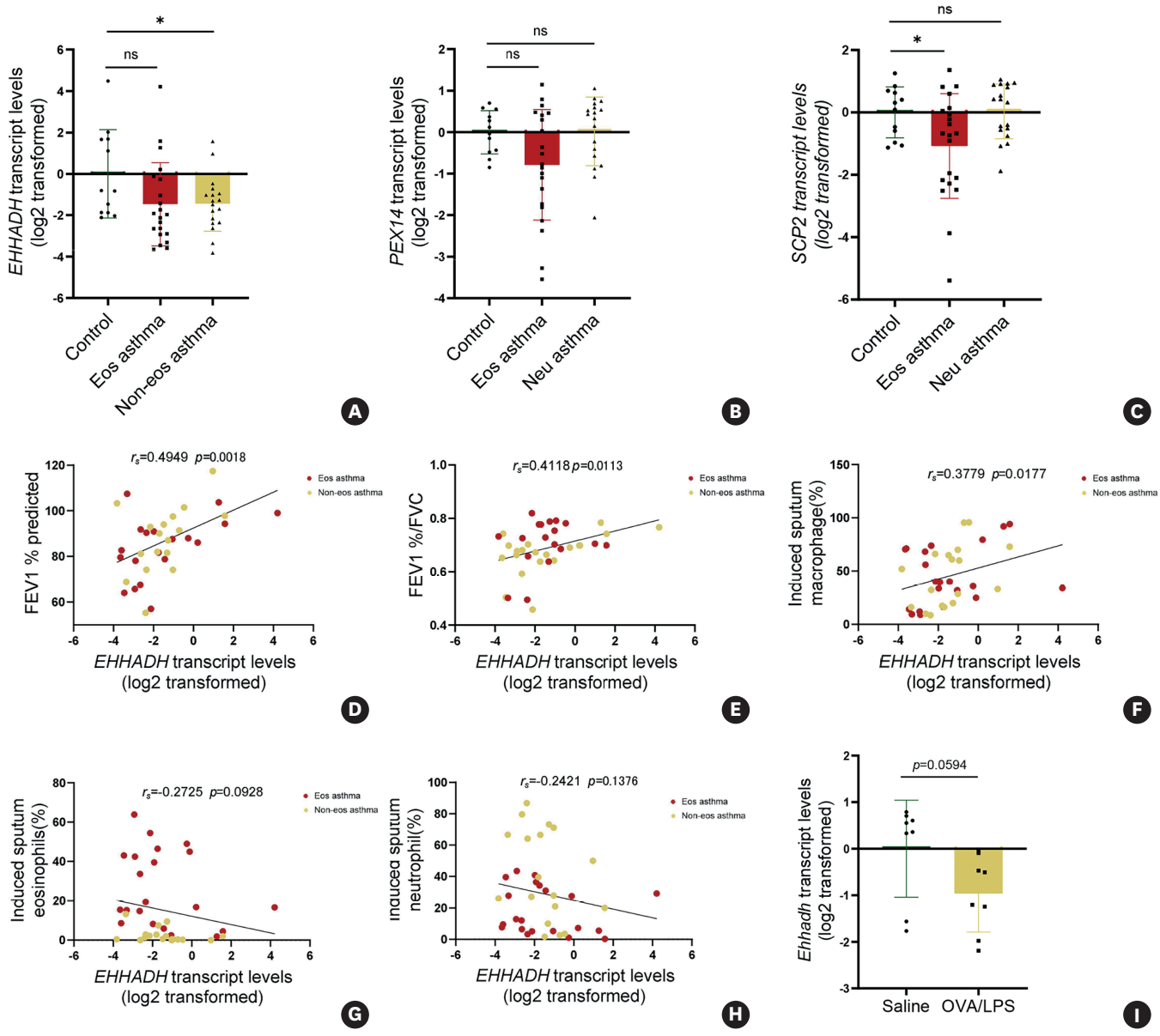

Fig. 2. EHHADH expression is decreased in sputum cells of non-EA and positively correlated with airflow limitation. (A-C) Detection of *EHHADH*, *PEX14*, *SCP2* mRNA level in sputum cells of control (n = 12), EA (n = 21) and non-EA (n = 18) using quantitative RT-PCR. The transcript levels were expressed as log2 transformed and relative to the median value for control group. (D-H) Spearman's correlation assays between *EHHADH* transcripts in sputum cells and FEV1% predicted, FEV1%/FVC, the proportion of macrophages, eosinophils, and neutrophils in induced sputum. (I) Detection of *Ehhadh* mRNA level in lung tissue from a mouse model of neutrophilia-dominant allergic airway inflammation using RT-PCR.
EHHADH, enoyl-CoA hydratase and 3-hydroxyacyl CoA dehydrogenase; PEX14, peroxisomal biogenesis factor 14; SCP2, sterol carrier protein 2; EA, eosinophilic asthma; RT-PCR, reverse transcription polymerase chain reaction; FEV1, forced expiratory volume in the first second; FVC, forced vital capacity; ns, not significant; OVA, ovalbumin; LPS, lipopolysaccharide.
*$P < 0.05$.

Furthermore, the relative fluorescence intensity of Ehhadh/Cd68 was significantly decreased in mice with neutrophilia-dominant allergic airway inflammation compared to control mice (**Fig. 4A and B**). The relative fluorescence intensity of Ehhadh/DAPI was also decreased (**Fig. 4C**). These findings suggest that the expression of EHHADH is downregulated in macrophages in non-EA.

https://doi.org/10.4168/aair.2025.17.1.111

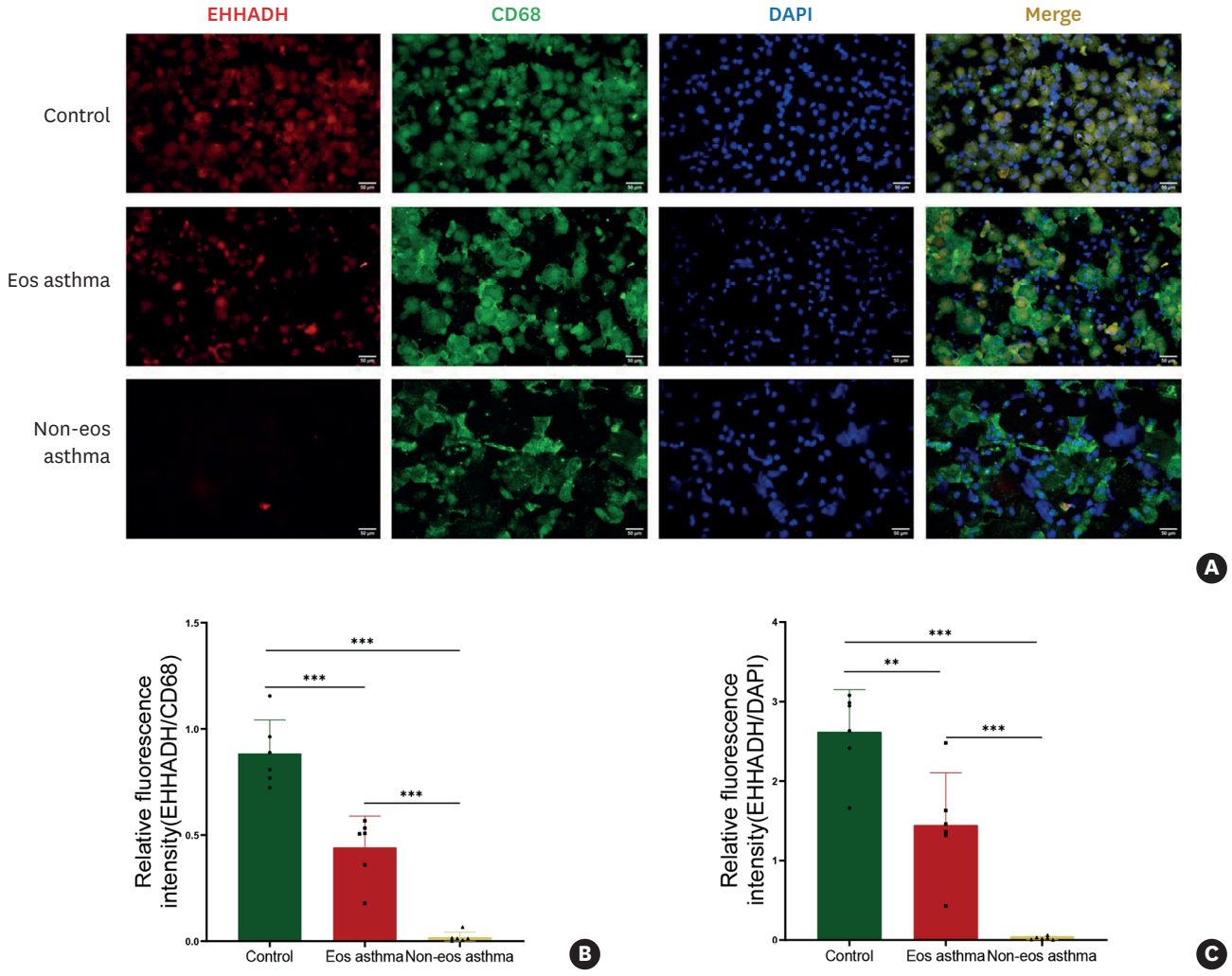

Fig. 3. The expression of EHHADH is decreased in BAL cells, especially in macrophages from non-EA patients. (A) Representative images of EHHADH and CD68 immunohistochemical staining in BAL cells from EA patients, non-EA patients and control subjects. (B, C) The relative fluorescence intensity of EHHADH/CD68 and EHHADH/DAPI in BAL cells was analyzed using ImageJ.
EHHADH, enoyl-CoA hydratase and 3-hydroxyacyl CoA dehydrogenase; BAL, bronchoalveolar lavage; CD68, cluster of differentiation 68; EA, eosinophilic asthma; DAPI, 4′,6-diamidino-2-phenylindole.
$^{**}P < 0.01$, $^{***}P < 0.001$.

EHHADH expression is downregulated in M1-like macrophages *in vitro*

Macrophage M1 polarization plays an important role in NA.[19] We investigated the expression of Ehhadh in mouse BMDMs stimulated with LPS, an inducer of M1 polarization. Western blotting showed that the protein level of Ehhadh was decreased significantly following LPS stimulation compared to unstimulated controls (**Fig. 5A-C**). Additionally, quantitative PCR results confirmed a similar reduction in *Ehhadh* mRNA levels in LPS-stimulated BMDMs compared to control cells (**Fig. 5D-F**). To validate the downregulation of EHHADH in M1-like macrophages in humans, we analyzed the dataset GSE40885, including transcriptional expression data of human alveolar macrophages stimulated by LPS. We found that the expression of EHHADH in human alveolar macrophages exposed to LPS was significantly decreased compared to those exposed to saline (**Supplementary Fig. S6B**). These findings collectively suggest that the expression of EHHADH is downregulated in macrophages undergoing M1 polarization.

https://doi.org/10.4168/aair.2025.17.1.111

Allergy, Asthma & Immunology Research AAIR

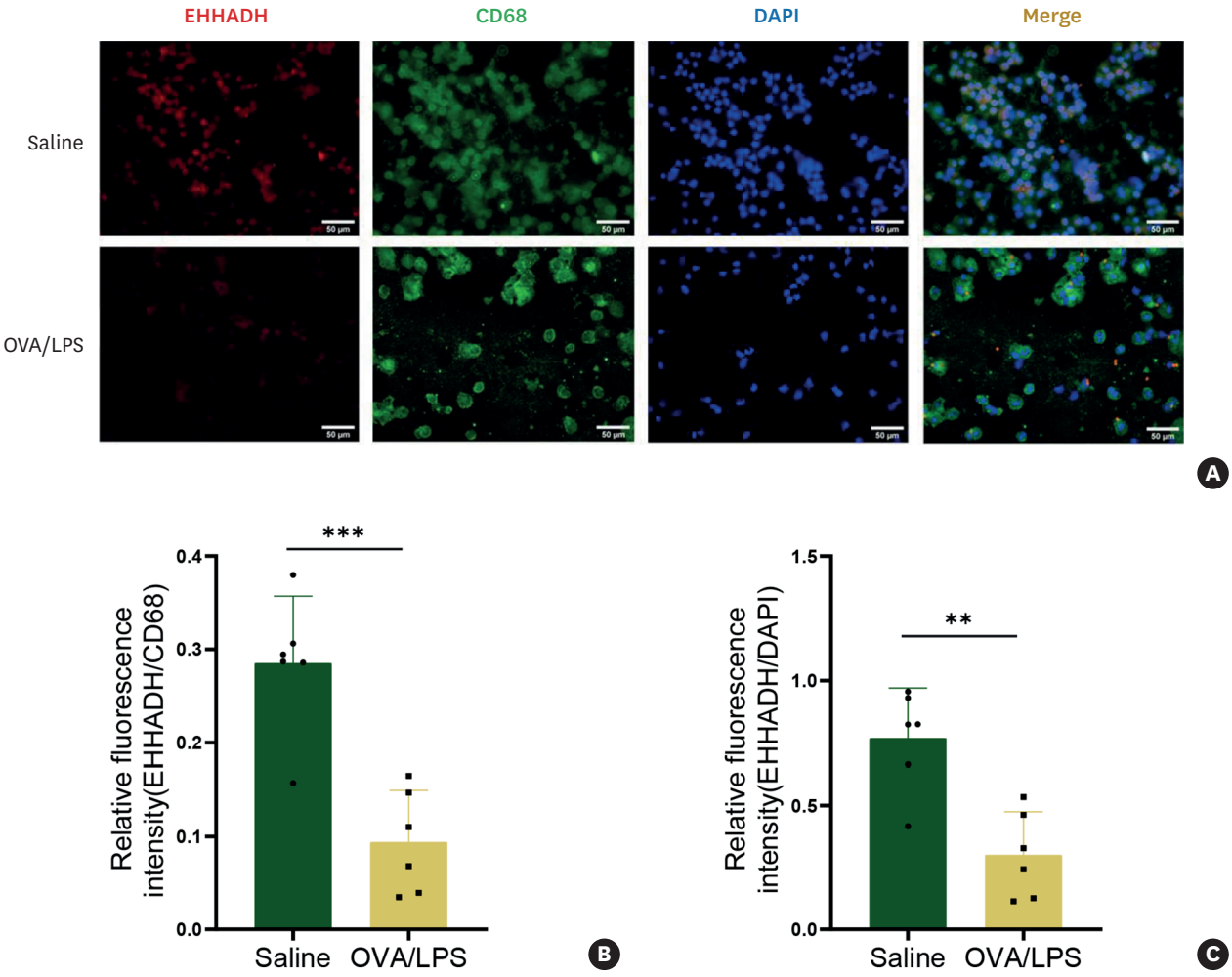

Fig. 4. The expression of Ehhadh in macrophages is decreased in a mouse model of neutrophilia-dominant allergic airway inflammation. (A) Representative images of Ehhadh and Cd68 immumohistochemical staining in BAL cells from mice with neutrophilia-dominant allergic airway inflammation and control mice. (B, C) The relative fluorescence intensity of Ehhadh/Cd68 and Ehhadh/DAPI in BAL cells was analyzed using ImageJ.
Ehhadh, enoyl-CoA hydratase and 3-hydroxyacyl CoA dehydrogenase; Cd68, cluster of differentiation 68; BAL, bronchoalveolar lavage; DAPI, 4′,6-diamidino-2-phenylindole; OVA, ovalbumin; LPS, lipopolysaccharide.
$^{**}P < 0.01$, $^{***}P < 0.001$.

Peroxisome pathway agonist fenofibrate inhibits macrophage M1 polarization

Given that EHHADH, SCP2, and PEX14 are all involved in the peroxisome pathway, we next analyzed the enrichment of this pathway in dataset GSE41863, which included the gene expression data of sputum cells from NA and EA patients. GSEA analysis revealed that the peroxisome pathway was significantly enriched in control and patients with EA compared to those with NA (**Fig. 6A and B**). Further examination of peroxisome pathway-related genes showed that most of these genes were significantly downregulated in patients with NA (**Fig. 6C**). Since peroxisomes play a key role in fatty acid metabolism, we also analyzed the enrichment of fatty acid metabolism pathway by GSEA. The results indicated that fatty acid metabolism pathway genes were significantly enriched in control subjects and patients with EA compared to those with NA (**Supplementary Fig. S8**).

To further investigate the relationship between the peroxisome pathway and macrophage M1 polarization, we treated BMDMs with a peroxisome pathway agonist, fenofibrate. Our

https://doi.org/10.4168/aair.2025.17.1.111

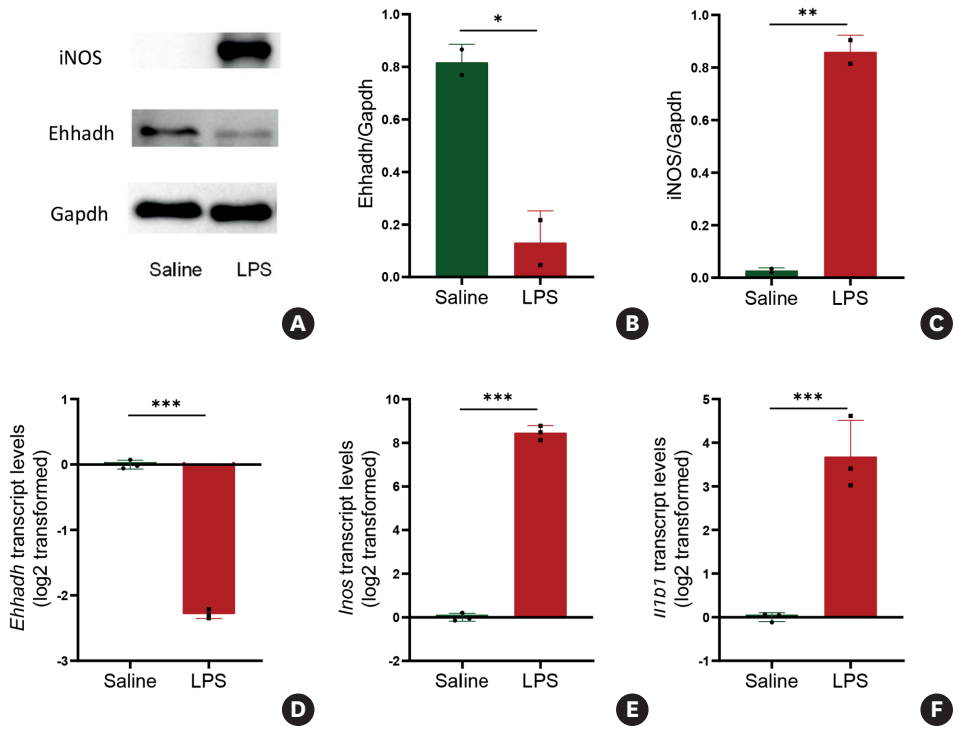

Fig. 5. EHHADH expression is downregulated in M1-like macrophages *in vitro*. (A) The protein levels of Ehhadh and iNOS in BMDM cells after exposure to LPS for 48 hours were determined by Western blotting. (B, C) A densitometry assay was performed using ImageJ. Ehhadh and iNOS protein levels were indexed to Gapdh. (D-F) The mRNA levels of *Ehhadh*, *Inos* and *Il1b* in BMDM cells after exposure to LPS for 48 hours were determined by RT-PCR. The transcript levels were expressed as log2 transformed and relative to the median value for the control group.
EHHADH, enoyl-CoA hydratase and 3-hydroxyacyl CoA dehydrogenase; iNOS, inducible nitric oxide synthase; BMDM, bone marrow-derived macrophage; LPS, lipopolysaccharide; Gapdh, glyceraldehyde 3-phosphate dehydrogenase; IL, interleukin; RT-PCR, reverse transcription polymerase chain reaction.
$^{*}P < 0.05$, $^{**}P < 0.01$, $^{***}P < 0.001$.

findings demonstrated that fenofibrate significantly inhibits LPS-induced macrophage M1 polarization (**Fig. 6D and E**). These results suggest that downregulation of the peroxisome pathway may contribute to macrophage M1 polarization and the pathogenesis of NA.

DISCUSSION

This study demonstrated that the peroxisome and fatty acid metabolism pathways are downregulated in NA. Furthermore, EHHADH, which encodes an enzyme of the peroxisomal beta-oxidation pathway, has been identified as a key molecular marker and is downregulated in NA or severe asthma. In our cohort of asthma patients, EHHADH expression was decreased in non-EA patients and is correlated with airflow limitation. In a mouse model of neutrophilia-dominant allergic airway inflammation, EHHADH was primarily expressed in macrophages and was found to be downregulated. In cultured mouse BMDM cells, EHHADH expression was decreased in LPS-induced M1-like macrophages.

Peroxisomes are membrane-enclosed organelles present in most eukaryotic cells.[20] They play a crucial role in various essential metabolic activities, including the synthesis and turnover of complex lipids. Specifically, peroxisomes are responsible for the β-oxidation of very-long-chain fatty acids, the α-oxidation of branched-chain fatty acids, and the synthesis of ether lipids. Besides, peroxisomes also contribute to the detoxification of reactive oxygen species, reactive nitrogen species and the metabolism of polyamines,

https://doi.org/10.4168/aair.2025.17.1.111

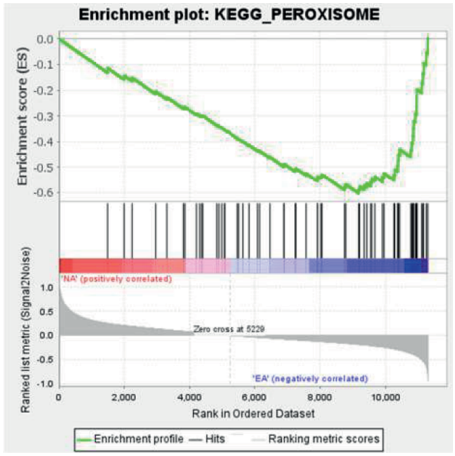

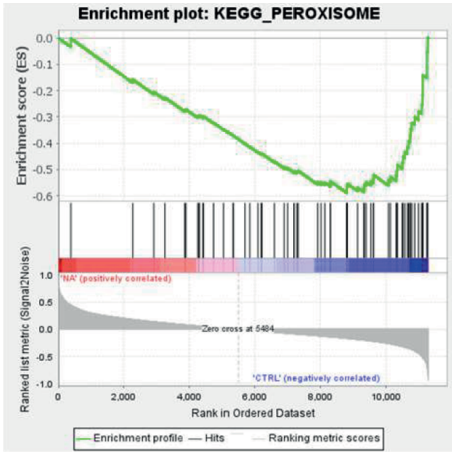

A

B

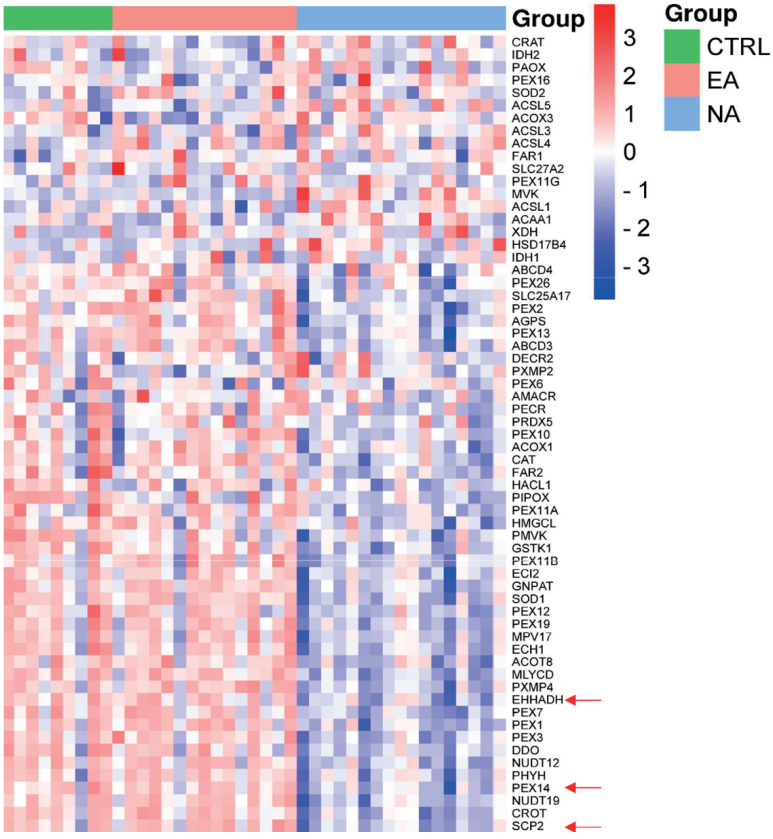

C

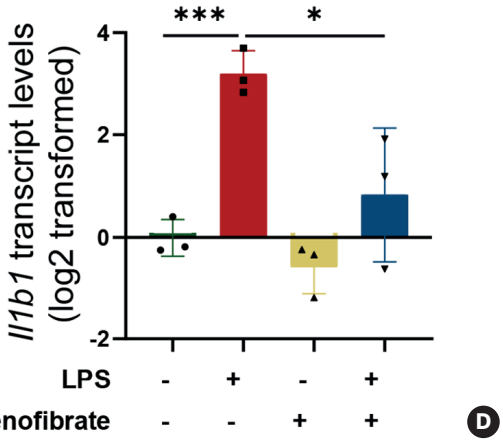

D

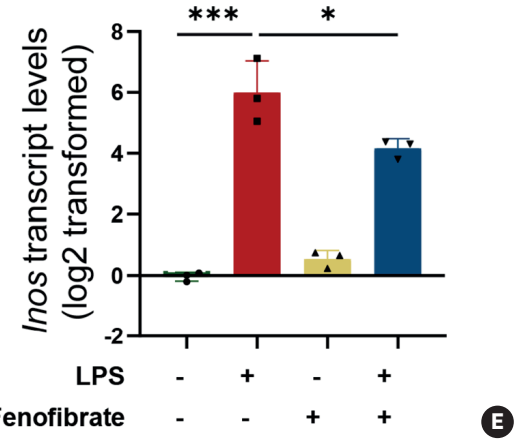

E

Fig. 6. Peroxisome pathway agonist fenofibrate inhibits macrophage M1 polarization. (A) GSEA plots of peroxisome pathway in NA and EA patients from dataset GSE41863. (B) GSEA plots of peroxisome pathway in NA patients and control subjects. (C) The heatmap of the peroxisome pathway gene sets in NA and EA patients, as well as control subjects. (D-E) Primary cultures of BMDMs were stimulated with LPS and/or fenofibrate for 48 hours. The mRNA levels of *Inos* and *Il1b* were determined by RT-PCR. The transcript levels were expressed as log2 transformed and relative to the mean value of the control group.
GSEA, Gene Set Enrichment Analysis; NA, neutrophilic asthma; EA, eosinophilic asthma; BMDM, bone marrow-derived macrophage; LPS, lipopolysaccharide; iNOS, inducible nitric oxide synthase; IL, interleukin; RT-PCR, reverse transcription polymerase chain reaction; KEGG, Kyoto Encyclopedia of Genes and Genomes; CTRL, healthy controls.
*P < 0.05, ***P < 0.001.

https://doi.org/10.4168/aair.2025.17.1.111

amino acids, and carbohydrates.[21] Peroxisomal β-oxidation is vital for the final step in the synthesis of immune-relevant polyunsaturated fatty acids, including docosahexaenoic acid (DHA) and eicosapentaenoic acid (EPA). DHA and EPA possess immunosuppressive and anti-inflammatory properties, regulating immune response pathways across various types of immune cells.[22] Moreover, induction of peroxisome proliferation in RAW 264.7 murine macrophages, primary murine alveolar and peritoneal macrophages through treatment with 4-phenyl butyric acid leads to a reduction in the expression of LPS-induced proinflammatory proteins, such as cyclooxygenase-2, tumor necrosis factor-α, and IL6 and IL12.[23]

We observed significant downregulation of peroxisome and fatty acid metabolism pathway-related genes in induced sputum samples from patients with NA compared to controls and those with EA. This suggests that impaired fatty acid metabolism, resulting from inhibition of the peroxisome pathway, may contribute to airway inflammation in NA. In support of our findings, Reinke and colleagues reported that fatty acid metabolism and β-oxidation pathways are inhibited in induced sputum samples from individuals with severe asthma.[24] Obese asthma patients usually exhibit neutrophilic airway inflammation. Scott and colleagues[25] found that obese asthma patients had higher levels of neutrophils in their sputum compared to non-obese patients, while the eosinophil levels were similar. Obesity is commonly associated with impaired fatty acid metabolism. Obesity impairs cellular metabolism, shifting dependence toward glucose oxidation and reducing fatty acid oxidation, which leads to increased fat deposition in skeletal muscle, liver, and other tissues. This reduction in fatty acid oxidation is a recognized risk factor for obesity. Obesity is also highly prevalent among individuals with severe asthma. These reports and our findings suggest that the downregulation of peroxisome and fatty acid metabolism pathways may contribute to the development of neutrophilic or severe asthma in obese individuals.

Peroxisome proliferator-activated receptor α is a key gene involved in the peroxisome pathway. Its agonist, fenofibrate, is widely used to reduce elevated cholesterol and triglyceride levels in plasma. Several studies have demonstrated that fenofibrate can inhibit OVA-induced eosinophilic airway inflammation, LPS/OVA-induced neutrophilic inflammation, and LPS-induced acute lung injury in mice.[26-28] However, the underlying mechanism remains unclear. Kim and colleagues reported a positive correlation between neutrophil percentages and M1 macrophage percentages in induced sputum of individuals with non-EA, suggesting a link between non-EA and M1 macrophage activation.[19] Another study showed that long-chain fatty acids can induce endoplasmic reticulum stress, increase mitochondrial reactive oxygen species, activate toll-like receptors, and promote M1 polarization of macrophages.[29] In this study, we found that fenofibrate significantly inhibited LPS-induced M1 polarization of BMDMs. Taken these reports and our findings together, activation of the peroxisome pathway may suppress airway inflammation by inhibiting M1 polarization in macrophages, particularly in NA.

EHHADH is a key enzyme in the peroxisomal β-oxidation of fatty acids, contributing to the fundamental function of peroxisomes.[30] EHHADH contains two distinct domains responsible for hydration and dehydrogenation activities, classifying it as a bifunctional enzyme.[31] Our bioinformatics analysis suggests that EHHADH may play a role in NA, as its expression in induced sputum showed a significant correlation with predicted FEV1%, indicating its association with airflow limitation in asthma. We observed reduced EHHADH expression in sputum macrophages from patients with non-EA. In addition, we found decreased EHHADH expression in LPS-induced M1-like macrophages. These findings suggest that EHHADH downregulation may contribute to impaired fatty acid metabolism and macrophage M1 polarization in NA.

https://doi.org/10.4168/aair.2025.17.1.111

Our study has several limitations. First, the sample size of our cohort of asthma patients is relatively small. Secondly, we included non-eosinophilic patients in our clinical cohort instead of NA patients because the number of NA patients is limited. Thirdly, the levels of fatty acids in the BALF supernatant of asthmatic patients were not measured. Finally, the effect of fenofibrate on fatty acid levels and airway neutrophilia was not assessed in the mouse model. Further investigation is needed to explore the relationship between NA and peroxisome/fatty acid metabolism.

In conclusion, EHHADH expression and the peroxisome metabolism pathway are downregulated in macrophages in patients with NA. This downregulation may contribute to macrophage M1 polarization and neutrophilic airway inflammation in asthma.

ACKNOWLEDGMENTS

We sincerely thank Cheng DT for sharing their data in Gene Expression Omnibus database. The work was supported by National Natural Science Foundation of China (grant 82170036), Key Research and Development Program of Hubei Province (grant 2024BCB042), Innovation and Translation Project of Tongji Hospital (grant 2023CXZH006).

SUPPLEMENTARY MATERIALS

Supplementary Table S1

Primers for RT-PCR

Supplementary Fig. S1

GO and KEGG pathway enrichment annotations of DEGs in dataset GSE41863. (A, B) Volcano plots showed the DEGs in comparison between EA vs. CTRL, and DEGs between EA vs. NA by the criteria $P < 0.05$, $|\log FC| > 1$. (C-E) The results of GO enrichment categories included BP, CC, and MF. (F) The results of KEGG pathway enrichment analyses.

Supplementary Fig. S2

The heatmap of IL6R, IL10, CSF3, CXCR2, CSF3R, CXCR1, and JAK3 in dataset GSE41863.

Supplementary Fig. S3

The 6GS is significantly increased in NA. (A) The expression value of 6GS in the dataset GSE41863. (B) 6GS including *CLC*, *IL1B*, *CXCR2*, *CPA3*, *DNASE1L3*, and *ALPL* were shown in the heatmap.

Supplementary Fig. S4

The expression of EHHADH and SCP2 is decreased in severe asthma. The expression value of (A) EHHADH, (B) PEX14, and (C) SCP2 in the dataset GSE76262, included induced sputum cell microarray data for control, moderate asthma, and severe asthma.

Supplementary Fig. S5

EHHADH expression is not correlated with FeNO or serum total IgE. The correlation assay between EHHADH levels in induced sputum and FeNO (A), serum total IgE (B).

https://doi.org/10.4168/aair.2025.17.1.111

Supplementary Fig. S6

EHHADH expression tend to be decreased in non-EA. (A) Detection of EHHADH mRNA level in BAL cells of control, EA and non-EA using RT-PCR. The transcript levels were expressed as log2 transformed and relative to the median value for the control group. (B) The expression value of EHHADH in the microarray dataset for human alveolar macrophages exposed to LPS (dataset GSE40885).

Supplementary Fig. S7

Cell counts for macrophages, eosinophils, lymphocytes, and neutrophils in BALF in a mouse model of neutrophilia-dominant allergic airway inflammation.

Supplementary Fig. S8

Fatty acid metabolism pathway is downregulated in NA. (A) GESA plots of fatty acid metabolism pathway in NA and EA group. (B) GSEA plots of fatty acid metabolism pathway in NA and control group.

REFERENCES

1. Lambrecht BN, Hammad H. The immunology of asthma. Nat Immunol 2015;16:45-56. PUBMED | CROSSREF
2. Tan LD, Alismail A, Ariue B. Asthma guidelines: comparison of the National Heart, Lung, and Blood Institute Expert Panel Report 4 with Global Initiative for Asthma 2021. Curr Opin Pulm Med 2022;28:234-44. PUBMED | CROSSREF
3. Chi-Leung D. The big 5 respiratory diseases give insight into respiratory health and beyond. Respirology 2023;28:496-7. PUBMED | CROSSREF
4. King GG, James A, Harkness L, Wark PA. Pathophysiology of severe asthma: we've only just started. Respirology 2018;23:262-71. PUBMED | CROSSREF
5. Tliba O, Panettieri RA Jr. Paucigranulocytic asthma: uncoupling of airway obstruction from inflammation. J Allergy Clin Immunol 2019;143:1287-94. PUBMED | CROSSREF
6. Taylor SL, Leong LE, Choo JM, Wesselingh S, Yang IA, Upham JW, et al. Inflammatory phenotypes in patients with severe asthma are associated with distinct airway microbiology. J Allergy Clin Immunol 2018;141:94-103.e15. PUBMED | CROSSREF
7. Pelaia G, Vatrella A, Busceti MT, Gallelli L, Calabrese C, Terracciano R, et al. Cellular mechanisms underlying eosinophilic and neutrophilic airway inflammation in asthma. Mediators Inflamm 2015;2015:879783. PUBMED | CROSSREF
8. Zhang X, Xu Z, Wen X, Huang G, Nian S, Li L, et al. The onset, development and pathogenesis of severe neutrophilic asthma. Immunol Cell Biol 2022;100:144-59. PUBMED | CROSSREF
9. Komlósi ZI, van de Veen W, Kovács N, Szűcs G, Sokolowska M, O'Mahony L, et al. Cellular and molecular mechanisms of allergic asthma. Mol Aspects Med 2022;85:100995. PUBMED | CROSSREF
10. Lee JW, Chun W, Lee HJ, Min JH, Kim SM, Seo JY, et al. The role of macrophages in the development of acute and chronic inflammatory lung diseases. Cells 2021;10:897. PUBMED | CROSSREF
11. Yunna C, Mengru H, Lei W, Weidong C. Macrophage M1/M2 polarization. Eur J Pharmacol 2020;877:173090. PUBMED | CROSSREF
12. Ross EA, Devitt A, Johnson JR. Macrophages: the good, the bad, and the gluttony. Front Immunol 2021;12:708186. PUBMED | CROSSREF
13. Shi B, Hao Y, Li W, Dong H, Xu M, Gao P. TIPE2 may target the Nrf2/HO-1 pathway to inhibit M1 macrophage-related neutrophilic inflammation in asthma. Front Immunol 2022;13:883885. PUBMED | CROSSREF
14. Saradna A, Do DC, Kumar S, Fu QL, Gao P. Macrophage polarization and allergic asthma. Transl Res 2018;191:1-14. PUBMED | CROSSREF
15. Okumoto K, Tamura S, Honsho M, Fujiki Y. Peroxisome: metabolic functions and biogenesis. Adv Exp Med Biol 2020;1299:3-17. PUBMED | CROSSREF

16. Wanders RJ, Vaz FM, Waterham HR, Ferdinandusse S. Fatty acid oxidation in peroxisomes: enzymology, metabolic crosstalk with other organelles and peroxisomal disorders. Adv Exp Med Biol 2020;1299:55-70. PUBMED | CROSSREF
17. Rodriguez-Perez N, Schiavi E, Frei R, Ferstl R, Wawrzyniak P, Smolinska S, et al. Altered fatty acid metabolism and reduced stearoyl-coenzyme a desaturase activity in asthma. Allergy 2017;72:1744-52. PUBMED | CROSSREF
18. Fricker M, Gibson PG, Powell H, Simpson JL, Yang IA, Upham JW, et al. A sputum 6-gene signature predicts future exacerbations of poorly controlled asthma. J Allergy Clin Immunol 2019;144:51-60.e11. PUBMED | CROSSREF
19. Kim J, Chang Y, Bae B, Sohn KH, Cho SH, Chung DH, et al. Innate immune crosstalk in asthmatic airways: innate lymphoid cells coordinate polarization of lung macrophages. J Allergy Clin Immunol 2019;143:1769-1782.e11. PUBMED | CROSSREF
20. Di Cara F, Savary S, Kovacs WJ, Kim P, Rachubinski RA. The peroxisome: an up-and-coming organelle in immunometabolism. Trends Cell Biol 2023;33:70-86. PUBMED | CROSSREF
21. Wanders RJ, Waterham HR. Biochemistry of mammalian peroxisomes revisited. Annu Rev Biochem 2006;75:295-332. PUBMED | CROSSREF
22. Radzikowska U, Rinaldi AO, Çelebi Sözener Z, Karaguzel D, Wojcik M, Cypryk K, et al. The influence of dietary fatty acids on immune responses. Nutrients 2019;11:2990. PUBMED | CROSSREF
23. Vijayan V, Srinu T, Karnati S, Garikapati V, Linke M, Kamalyan L, et al. A new immunomodulatory role for peroxisomes in macrophages activated by the TLR4 ligand lipopolysaccharide. J Immunol 2017;198:2414-25. PUBMED | CROSSREF
24. Reinke SN, Naz S, Chaleckis R, Gallart-Ayala H, Kolmert J, Kermani NZ, et al. Urinary metabotype of severe asthma evidences decreased carnitine metabolism independent of oral corticosteroid treatment in the U-BIOPRED study. Eur Respir J 2022;59:2101733. PUBMED | CROSSREF
25. Scott HA, Gibson PG, Garg ML, Wood LG. Airway inflammation is augmented by obesity and fatty acids in asthma. Eur Respir J 2011;38:594-602. PUBMED | CROSSREF
26. Alhirmizi IA, Uysal F, Arslan SO, Özünlü SA, Koç A, Parlar A, et al. Fenofibrate attenuates asthma features in an ovalbumin-induced mouse model via suppressing NF-κB binding activity. Respir Physiol Neurobiol 2023;314:104083. PUBMED | CROSSREF
27. Elaidy SM, Essawy SS, Hussain MA, El-Kherbetawy MK, Hamed ER. Modulation of the IL-23/IL-17 axis by fenofibrate ameliorates the ovalbumin/lipopolysaccharide-induced airway inflammation and bronchial asthma in rats. Naunyn Schmiedebergs Arch Pharmacol 2018;391:309-21. PUBMED | CROSSREF
28. Cui H, Xie N, Banerjee S, Ge J, Guo S, Liu G. Impairment of fatty acid oxidation in alveolar epithelial cells mediates acute lung injury. Am J Respir Cell Mol Biol 2019;60:167-78. PUBMED | CROSSREF
29. Namgaladze D, Brüne B. Macrophage fatty acid oxidation and its roles in macrophage polarization and fatty acid-induced inflammation. Biochim Biophys Acta 2016;1861:1796-807. PUBMED | CROSSREF
30. Yang G, Sun S, He J, Wang Y, Ren T, He H, et al. Enoyl-CoA hydratase/3-hydroxyacyl CoA dehydrogenase is essential for the production of DHA in zebrafish. J Lipid Res 2023;64:100326. PUBMED | CROSSREF
31. Ranea-Robles P, Violante S, Argmann C, Dodatko T, Bhattacharya D, Chen H, et al. Murine deficiency of peroxisomal L-bifunctional protein (EHHADH) causes medium-chain 3-hydroxydicarboxylic aciduria and perturbs hepatic cholesterol homeostasis. Cell Mol Life Sci 2021;78:5631-46. PUBMED | CROSSREF